Proceedings of the 10th World Congress on Electrical Engineering and Computer Systems and Sciences (EECSS'24)
Barcelona, Spain – August 19 - 21, 2024
Paper No. ICBES 138
DOI: 10.11159/icbes24.138

Reactive Inkjet Printed Silk Stirrers for Rapid Medical Diagnosis

Deepum Nrupeshbhai Patel and Khushi Issuar
The University of Sheffield
S10 2TN, Sheffield, United Kingdom
dpatel11@sheffield.ac.uk; kissuar1@sheffield.ac.uk

Abstract **-** Medical diagnostic kits play a vital role in the quick and precise identification of diseases; however, their test times are often limited by the efficiency of molecular interactions between target molecules and binding sites. This research project aims to enhance the performance of medical diagnostic kits by developing surface tension-powered stirring devices using reactive inkjet printing technology which will aim to increase the rate of successful collisions between these target molecules and the binding sites.

The ink utilised in this study comprises of silk fibroin, a structural protein derived from the silk cocoon of the Bombyx mori. Silk fibroin possesses versatile biological applications, making it an ideal material for biomedical purposes. The ink is created by subjecting the fibroin fibres to a series of processes, including degumming to remove sericin layers and obtaining Regenerated Silk Fibroin (RSF) through various processes such as Dissolution and Dialysis. Methanol exposure is employed to induce the solidification of the printed structure through the formation of secondary protein structures, specifically Beta-pleated sheets.

To facilitate controlled rotation and stirring, Polyethylene Glycol (surfactant) is strategically printed at designated regions, referred to as motor regions. The stirrers are driven by surface tension gradients through the use of a surfactant (Marangoni effect), which elucidates the mechanism behind the induced rotation. Two different stirrer designs were tested, both of which exhibited significant motion. This innovative approach aims to improve reagent and sample mixing within diagnostic kits, thereby enhancing the accuracy and speed of medical diagnosis. The integration of reactive inkjet printed silk micro stirrers holds great promise for advancing the field of rapid medical diagnosis, contributing to more effective disease detection and timely intervention. These stirring devices are also valuable in industries requiring homogenous mixing at small scales (nanoparticle synthesis), immunoassay testing in medical diagnosis kits and lab-on-chip applications.

Keywords**:** Reactive inkjet printing, Regenerated Silk Fibroin, Marangoni effect, microstirrer

1 Introduction

Diseases can be quickly and accurately diagnosed using medical diagnostic kits. However, they are limited by the rate of successful collisions between target molecules and binding sites, hence significantly affecting the success rates of the kits. Effective reagent and sample mixing can improve the accuracy, sensitivity and speed of these tests. Conventional techniques used to agitate small volumes of solution often require external power, leading to compatibility concerns with diagnosis kits and medical applications.[1] In this paper, surface tension-powered stirring devices have been developed based on the Marangoni effect capable of carrying out micro-scale mixing motion. By improving the reagent and sample mixing, the effectiveness of the medical diagnosis kits is increased. The production method uses reactive inkjet printing technology for precise printing of the stirrers.

The structural protein of the silk cocoon, known as silk fibroin, serves as the primary component for producing the ink required for printing the stirrers. The excellent mechanical properties, biocompatibility and biodegradability qualities of the silk make it a popular material option, especially for biological applications.[1][2] This is because it provides mechanical strength and minimises environmental concerns. To get fibroin fibre appropriate for biomedical applications, operations to remove the sericin layer (glue-like proteins) that surrounds the fibroin fibres must be carried out (degumming) followed by a few extra procedures to obtain Regenerated Silk Fibroin (RSF) which is used as the main component of ink to print the devices.

To solidify the printed structure (fibroin coils), the RSF is treated with methanol. The exposure to methanol stimulates the formation of insoluble secondary protein structures, beta-pleated sheets, which provide the stirrers its structural integrity and shape. Polyethylene glycol (specifically PEG400), which acts as a surface active agent will then be printed at specific regions (motor regions) to give rise to regular rotational motion which is explained by the Marangoni effect. The Marangoni effect is the mass transfer between the interface of two fluids due to the surface tension gradient.[3] In comparison to the

catalytically driven devices, the Marangoni effect has several advantages, hence is chosen as the preferred method for this study. These include no requirements for additional external chemicals to 'fuel' the rotation hence reducing the risks of contamination or side effects and potentially providing a faster rotation speed.[3] The addition of the PEG400 in the inks is crucial for generating surface tension gradients by the leaching out of the PEG400 from the motor regions.

Reactive inkjet printing, employing piezoelectric jetting nozzles, was utilised in the fabrication process. This printing technique shares similarities with 3D printing. Notably, within the context of manufacturing stirring devices, it offers several attractive features. One such feature is the ability to accurately and digitally define the overall shape of the device, akin to 3D printing methodologies. Additionally, this technique enables precise deposition of motion-producing chemical components. The former feature facilitates the creation of devices with shapes and sizes conducive to fluid mixing in their vicinity, while the latter allows for potential control over the trajectory of the device.

2 Materials and Methods

Silk cocoons utilised to produce regenerated silk fibroin solution contain a protein glue-like layer called sericin that protects the silk fibres. To isolate the silk fibroin, a degumming process is used involving boiling the cocoons in sodium carbonate solution to dissolve the sericin, resulting in a weight loss of approximately 30%. The silk fibroin fibres extracted from the degumming process are transformed into a solution via dissolution utilising Ajisawa's reagent, which is preferred over the use of Lithium Bromide (LiBr) approach due to its cost-effectiveness, shorter processing time, and elimination of LiBr use. Ajisawa's reagent is composed of 3 part-solution containing deionised water, ethanol and calcium chloride in a molar ratio of 1:8:2, is used to dissolve the silk fibres, producing a yellow viscous liquid known as the regenerated silk fibroin solution (RSF).[4] RSF is further purified through the dialysis process to remove the remaining unwanted impurities such as salt and solutes, leaving behind the RSF and silk fibres. The process involves running the RSF solution in a dialysis tube of molecular weight cutoff (MWCO) of 3,500 for at least 30 hours with at least five water changes. Conductivity measurements are taken every 20 minutes to ensure the reproducibility of results until the conductivity is below 10µS to confirm complete dialysis. Further centrifugation is performed on the solution to remove the remaining undissolved silk fibres and foreign particles. The collected supernatant is stored at 4°C for the prevention of sol-gel transition or solidification and to ensure a longer window for printing. Several changes were implemented from the standard approach, such as designing and printing clamps for the dialysis treatment to optimise and shorten the process and reduce the wastage of the RSF solution.

3 Designing of Stirrers

Using Excel, an array of functions was used to plot the coordinates of the dots relative to the pre-defined centre. This made it easy to modify distance values at later stages when finding optimal distances to get good shape formation. The PEG_{400} (surfactant) was introduced in very specific locations of the stirrer, hence creating an engine or motor region of the stirrer that would power the device.

Motor region doped with PEG_{400}

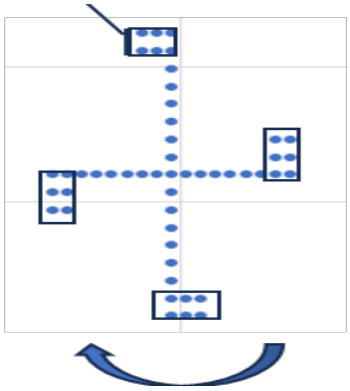

Figure 1 shows design of 4 Arm stirrer with blue arrow showing intended direction of rotation.

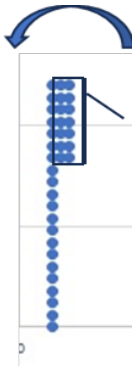

Motor region doped with PEG_{400}

Figure 2 shows design of Single Arm stirrer with blue arrow showing intended direction of rotation.

4 Printing

Three piezoelectric jetting nozzles of the following diameters: 40μm, 80μm, and 80μm are used to print the methanol solution, RSF and RSF with PEG solution, respectively. As each nozzle possessed distinct parameters, precise adjustments were necessary to achieve the desired outcome of producing elongated, fine droplets. These adjustments were controlled through proprietary software developed in-house.

To prepare the ink to be used in the printer:

- RSF solution diluted to 40mg/ml using filtered deionized water (used to make the main structure of the stirrer and is printed through a 40μm nozzle)
- RSF and PEG 400 solution of concentration 40mg/ml and 12mg/ml respectively (used to make the motor regions and is printed using an 80μm nozzle)
- Brillant blue in Methanol

Figure 2 shows an example of good droplet formation.

Methanol was chosen to induce the conversion of fibroin coils to beta-pleated sheets (secondary protein structures), thereby enhancing rigidity. The inclusion of Brilliant Blue dye served to augment contrast, aiding in device tracking.

Following the loading of the inks into the reservoirs, back pressure was adjusted to ensure that the ink did not drip out of the nozzle. Nitrogen gas was the preferred gas to pressurise the system due to its ability to minimise the likelihood of the RSF solutions undergoing gelation.

Figure 3 shows skewed droplets before calibration.

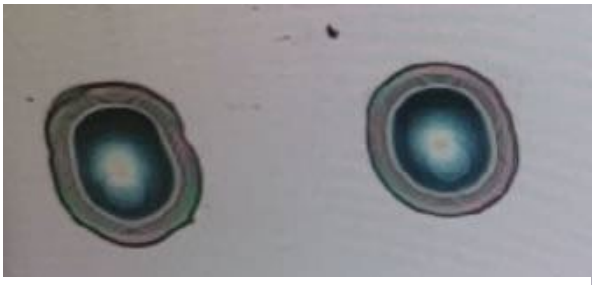

Figure 4 shows aligned droplets after calibration.

Nozzles were checked if their jetting positions were calibrated through a test involving the printing of an array of dots. The calibration parameters for each nozzle were then adjusted accordingly based on test outcomes.

The designed array, detailed in the previous section, is then imported into an in-house made control software where parameters such as thickness or number of layers and the number of drops corresponding to a dot in the design array can be adjusted, after which the printing process could be initiated onto a clean silicon wafer.

A 200-layer device that seemed optimal with 2 drops per dot was found to be optimal where the structure was sound and strong enough to withstand detachment from the silicon wafer without breakage.

Note: Extended periods of inactivity led to the drying and subsequent clogging of RSF solution-containing ink within the nozzles. The use of a micro-swab moistened with deionized water to dissolve the silk would solve the issue. In severe cases, a saturated solution of Lithium Bromide was employed to alleviate nozzle blockages. Furthermore, the presence of minute foreign particles necessitated the use of a vacuum, facilitated by a custom adapter connected to a syringe, in conjunction with a sonicator to fragment the particles for easy removal. However, the use of the sonicator was minimised due to its potential to cause slight damage to the nozzle surface.

Figure 5 shows total blockage of nozzle

5 Detachment and Data Acquisition

The main challenge at this stage was to find a way to detach the devices from the wafer without damaging the structures. Additionally, it was important to prevent loss of the PEG, this meant the use of any solution was not ideal, otherwise, the activity of the stirrer would be severely reduced.

An effective method was to place the wafer with the devices in a closed petri dish with some solid Calcium Chloride as a desiccant. The setup is then placed in an oven set at 70°C, followed by a brief exposure to a freezer.

Due to the rapid temperature changes and different rates of thermal contraction, the devices were much softer and easier to peel off using a flat blade.

It was observed that solely warming the devices increased their brittleness, leading to structural fracturing during detachment attempts.

To quantitatively assess the performance of the stirrers, high-resolution video was captured and used to digitally track the rotational motion of the devices. This was done by placing a clean glass petri dish under a camera with a cool white LED backlight and filling the petri dish with de-ionised water. Attention was paid to ensure that the water surface remained level with the brim of the dish, preventing the devices from being pulled to the centre or the walls during the video capture process.

The camera was set to capture 5400 frames at 60 frames per second to record a 90s video. To improve the contrast, it was better to turn off the room lights thereby eliminating potential colour aberrations or flickering.

The stirrers were gently placed on the surface of the water and once the motion of the device had stabilised, the video-capturing process was initiated. At the end of the capture, a **.pds** file was generated. This .pds file was then converted to an .avi file. The video was then imported into proprietary tracking software developed in-house, where individual devices were identified through user-defined boxes. The software conducted frame-by-frame analysis, employing pattern-matching algorithms to track device motion.

Post-tracking, positional data generated by the software were used to calculate key performance metrics such as the Mean Square Displacement Velocity (MSD Velocity), Mean Velocity of Centre and Total Distance Travelled.

Note: To get quantitative data, the tracking software was calibrated. This involved finding a length-per-pixel ratio using a ruler under identical magnification and focal length settings, thus providing a basis for precise quantitative analysis.

6 Results and Discussion

The two designs were created to have different stirring characteristics.

With the 4 Arm stirrer, a higher rpm was expected while spinning at a stationary point, as it had 4 engines (localised regions doped with PEG 400), thus producing a higher propulsion force.

For the Single Arm Stirrer, a lower rpm was expected due to its asymmetrical design and only one engine.

The results suggest that we were successful in creating active stirrers, however, the performances of each stirrer differed from our predicted behaviours outlined above. The mass of the stirrers may have contributed to this, whereby, the 4 arm stirrer was larger and thus heavier compared to the single-arm stirrer. Additionally, the 4 Arm Stirrer had a more pronounced rotation about a central point rather than rotating about its centre. The rpm was determined by counting the number of peaks in the Particle Orientation Graphs (shown).

Each class of stirrer exhibited 2 types of motion:

- 4 Arm Stirrer: rotation about a fixed point; rotation about a changing point.
- Single Arm Stirrer: rotation about a central point; irregular rotation with random changes in rotation direction.

Sample results:

4 Arm Stirrer - Rotation about a moving point

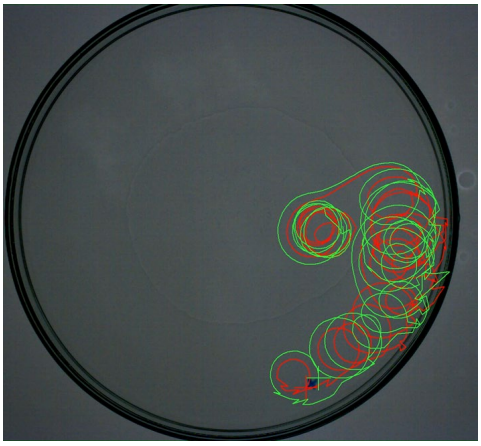

Figure 6 shows dual tracked image of 4 Arm stirrer.

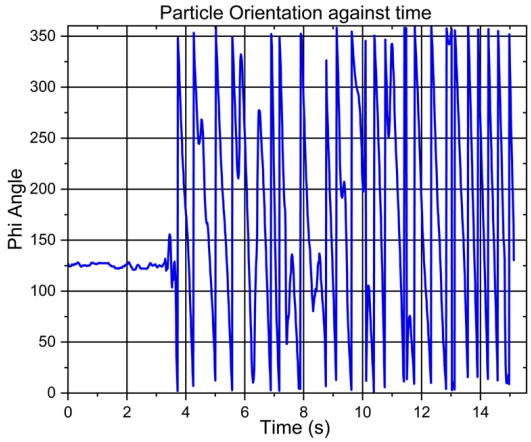

Figure 7 shows graph of particle orientation against time of 4 Arm stirrer.

Table 1 shows key results such as tracked speed and RPM.

Mean Vel. Track A (mm/s)	Mean Vel. Track B (mm/s)	Mean Vel. Centre of Mass (mm/s)	RPM
57.3	66.9	43.8	180

4 Arm Stirrer - Rotation about a fixed point

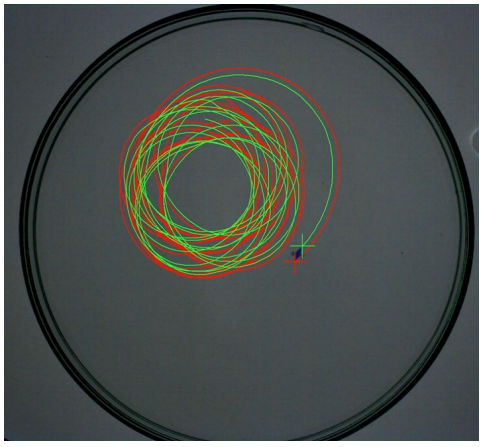

Figure 8 shows dual tracked image of 4 Arm stirrer.

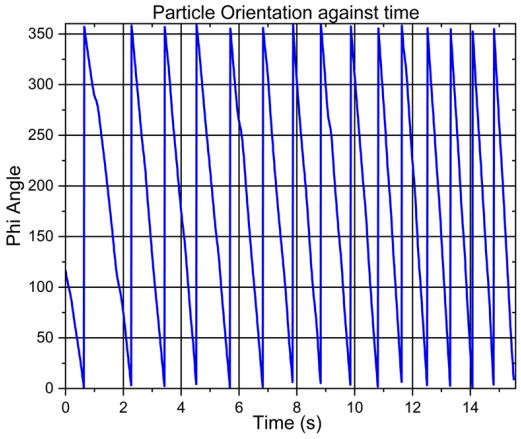

Figure 9 shows graph of particle orientation against time of 4 Arm stirrer.

Table 2 shows key results such as tracked speed and RPM.

Mean Vel. Track A (mm/s)	Mean Vel. Track B (mm/s)	Mean Vel. Centre of Mass (mm/s)	RPM
95.2	89.8	89.1	60

Single Arm Stirrer – Chaotic Rotation

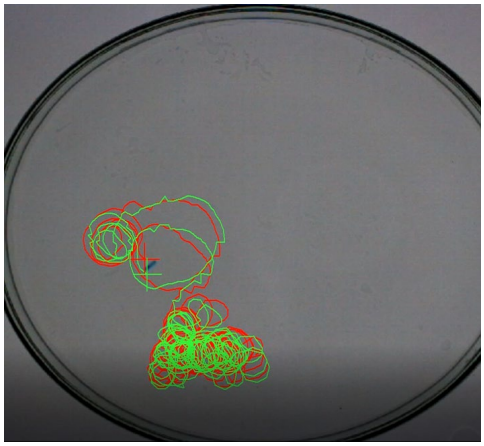

Figure 10 shows dual tracked image of Single Arm Stirrer

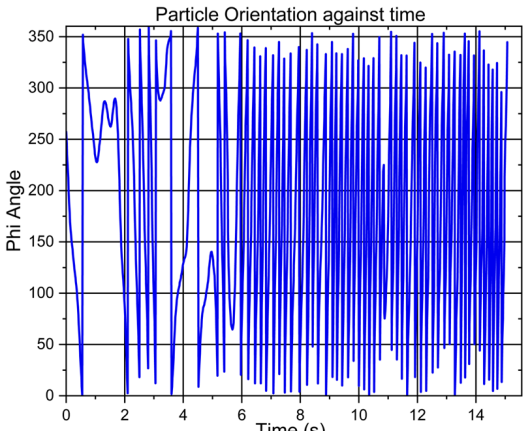

Figure 11 shows graph of particle orientation against time of Single Arm stirrer.

Table 3 shows key results such as tracked speed and RPM.

Mean Vel. Track A (mm/s)	Mean Vel. Track B (mm/s)	Mean Vel. Centre of Mass (mm/s)	RPM
52.2	47.9	21.0	150-300

Single Arm Stirrer – Rapid Regular Rotation

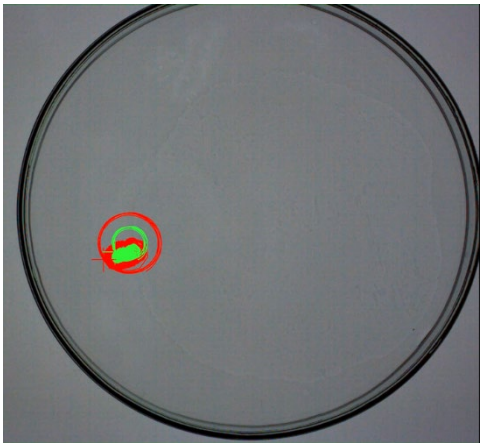

7

Figure 12 shows dual tracked image of Single Arm Stirrer.

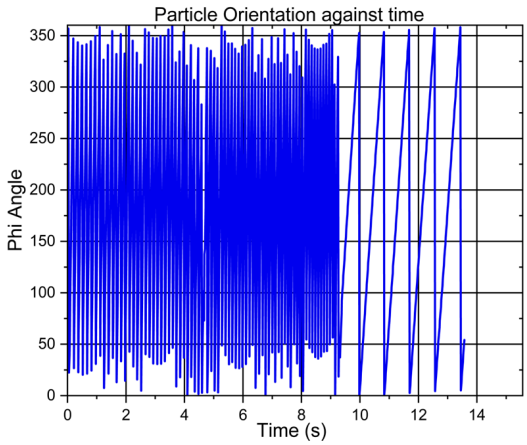

Figure 13 shows graph of particle orientation against time of Single Arm stirrer.

Table 4 shows key results such as tracked speed and RPM.

Mean Vel. Track A (mm/s)	Mean Vel. Track B (mm/s)	Mean Vel. Centre of Mass (mm/s)	RPM
34.5	19.4	15.5	540

Observations revealed occasional tracking inconsistencies as the software accidentally recorded the reflection of the stirrer against the glass wall of the petri dish.

It is important to mention that the number of samples assessed exceeded those shown above. The recorded activities encompassed the two types of motion illustrated for each stirrer, along with chaotic/random motion (results that were omitted). The erratic motion observed may be due to stirrer damage incurred during detachment. This necessitates the development of a more refined detachment technique to enhance the result's consistency. These findings serve as proof of concept that microstirrers can be autonomously powered, harnessing the Marangoni effect.

8 Conclusion

This study demonstrates the utilisation of the reactive inkjet printer to produce micro-scale silk stirrers employing the Marangoni effect. Data considering mean velocity for tracks A and B, centre mass, and rotations per minute (RPM) were collected for two types of stirrer shapes: single-arm and four-arm stirrers. The results reveal that the four-arm stirrer appears to be more suitable for larger well sizes due to its capacity to cover wider areas, while the single-arm stirrer is more suited for small well sizes. Regarding the rotation speed, the 4-arm stirrer ranged from 60-300 rpm, whereas the single arm ranged from 300-540 rpm, making it preferable for mixing applications, specifically medical kits.

A challenge experienced was the attachment of stirrers to the wall of the container when in proximity to the edges. Future tests are required to be carried out in the actual wells of medical kits (such as the immunoassay kits) to see if this is a common recurring problem.

Overall, this study presents the rotation results achieved for the two stirrer designs employing the Marangoni effect to see their potential use for enhancing rapid medical diagnosis kits by increasing their sensitivity, accuracy, and speed.

Acknowledgements

We are thankful to Dr David Alexander Gregory and Dr Stephen Ebbens for their invaluable guidance and support throughout the research project. We are also grateful to The University of Sheffield for providing us with this opportunity to participate in this project.

References

[1] Y. Zhang, D. A. Gregory, Y. Zhang, P. J. Smith, S. J. Ebbens, and X. Zhao, “Reactive Inkjet Printing of Functional Silk Stirrers for Enhanced Mixing and Sensing,” *Small*, vol. 15, no. 1, Dec. 2018, doi: https://doi.org/10.1002/smll.201804213.

[2] A. B. Li, J. A. Kluge, N. A. Guziewicz, F. G. Omenetto, and D. L. Kaplan, “Silk-based stabilization of biomacromolecules,” *Journal of Controlled Release*, vol. 219, pp. 416–430, Dec. 2015, doi: https://doi.org/10.1016/j.jconrel.2015.09.037.

[3]“Marangoni Effect-an overview |ScienceDirect Topics’’ *www.sciencedirect.com*. https://www.sciencedirect.com/topics/chemistry/marangoni-effect

[4]A. Ajisawa, “Dissolution of silk fibroin with calciumchloride/ethanol aqueous solution,” *The Journal of Sericultural Science of Japan*, vol. 67, no. 2, pp. 91–94, 1998, doi: https://doi.org/10.11416/kontyushigen1930.67.91.